Yokoyama et al. Int J Clin Cardiol 2015, 2:2
ISSN: 2378-2951

International Journal of
Clinical Cardiology

Research Article: Open Access

Influence of MRI-Conditional Cardiac Pacemakers on Quality and Interpretability of Images Acquired in 1.5-T Cardiac MRI

Kenichi Yokoyama[1]*, Toshiya Kariyasu[1], Shigehide Kuhara[2], Masamichi Imai[1], Rieko Ishimura[1] and Toshiaki Nitatori[1]

[1]*Department of Radiology, Kyorin University School of Medicine, Japan*

[2]*Clinical Application Research Center, Toshiba Medical Systems Corporation, Japan*

***Corresponding author:** *Kenichi Yokoyama, Department of Radiology, Kyorin University School of Medicine, 6-20-2 Shinkawa, Mitaka-shi, Tokyo 181-8611, Japan, Tel: +81-422-47-5511, Fax: +81-422-76-0361, E-mail: yokoyama@ks.kyorin-u.ac.jp*

Abstract

Purpose: The influence of MRI-conditional cardiac pacemakers on the quality and interpretability of images acquired in cardiac MRI (CMR) examinations was retrospectively investigated.

Materials and methods: The subjects in this study were 12 patients (7 men and 5 women, mean age: 68.4 ± 8.7 years) with MRI-conditional cardiac pacemakers who underwent CMR examinations at our institution between July 2013 and December 2014. Two readers graded the quality of the acquired cine images, fat-suppressed black blood T2-weighted images, and late gadolinium enhancement (LGE) images. The extent of the artifacts caused by the implantable pulse generator (IPG) and the size of the artifacts caused by the leads were also measured.

Results: All CMR examinations were performed safely. Image quality and interpretability were acceptable for the analysis of cardiac function and the evaluation of myocardial edema, scarring, and fibrosis, although deterioration of uniformity within the lumens due to magnetic field in homogeneity, artifacts from the leads (particularly those covering the left ventricular septal wall), and artifacts from the IPGs (particularly those covering the left ventricular anterior wall) were observed.

Conclusion: CMR can be performed safely in patients with MRI-conditional cardiac pacemakers, and images of sufficient quality for the assessment of cardiac anatomy and function can be obtained.

Keywords

Cardiac, MRI-conditional, Pacemaker, Sarcoidosis

Introduction

More than 2,000,000 patients in the United States have a permanent cardiac pacemaker, and an additional 3,000,000 patients meet the criteria for implantable cardioverterde fibrillator (ICD) implantation [1]. In Japan, approximately 250,000 patients have implanted cardiac implantable electronic devices (CIEDs), including pacemakers and ICDs. Given the advancing age of the population and the expanding indications for pacing and prophylaxis of ventricular arrhythmias, the number of patients with CIEDs will likely continue to increase [2,3]. It is estimated that 50% to 75% of this increasing population of patients with CIEDs will require a magnetic resonance imaging (MRI) examination at some point after implantation [4]. Given that 85% of all patients with CIEDs have one or more comorbidities, facilitating comprehensive multispecialty care is important [4,5].

MRI makes the early detection of medical conditions possible and offers important advantages over other imaging technologies, including the absence of ionizing radiation, excellent soft tissue resolution, and discrimination in any imaging plane [6]. MRI is recommended for the workup of many neurological, oncologic, and musculoskeletal diseases because of its unmatched ability to accurately visualize soft tissue. The presence of CIEDs, however, had been considered to be a contraindication to MRI [7-10], and device manufacturers had warned against MRI procedures for patients with such devices [11-13].

Recently, advances in cardiac device technology and MR-specific developments have led to the introduction of MRI-conditional CIEDs, providing more diagnostic options for patients with such devices [14]. In Japan, an MRI-conditional pacemaker was introduced in October 2012, and many MRI-conditional CIEDs are currently available. Patients with such MRI-conditional CIED scan safely undergo MRI examinations under certain conditions. While many of these examinations will be non-cardiac, cardiac MRI (CMR) is being performed with increasing frequency in these patients, as it allows for unparalleled assessment of morphology, function, and viability.

CMR is considered to be useful for identifying the causes of complete atrioventricular block, which is an indication for cardiac pacemaker implantation, and the causes of ventricular tachycardia (VT) and nonsustained VT, which are important indications for ICD implantation. One of the major diseases responsible for these abnormalities is cardiac sarcoidosis. Myocardial involvement of sarcoidosis is observed more frequently in Japan than in the United States or European countries and is responsible for the majority of deaths from sarcoidosis. It has been reported in Japan that cardiac

ClinMed
International Library

Citation: Yokoyama K, Kariyasu T, Kuhara S, Imai M, Ishimura R, et al. (2015) Influence of MRI-Conditional Cardiac Pacemakers on Quality and Interpretability of Images Acquired in 1.5-T Cardiac MRI. Int J Clin Cardiol 2:030

Received: April 10, 2015: **Accepted:** April 22, 2015: **Published:** April 24, 2015

Table1: Clinical and MR findings in 12 patients withMRI-conditional CIEDs

No.	Age/Sex	History	Clinical diagnosis	MR findings	CIED
1	50/M	Complete AV block	Cardiac sarcoidosis susp.	Cardiac sarcoidosis	Med
2	69/M	Complete AV block	Cardiac sarcoidosis susp.	Cardiac sarcoidosis	Med
3	67/F	Complete AV block	Cardiac sarcoidosis susp.	N/A	Med
4	70/M	Complete AV block	Cardiac sarcoidosis susp.	N/A	SJM
5	78/M	Complete AV block	Cardiac sarcoidosis susp.	N/A	Med
6	65/F	Sick sinus syndrome	Secondary cardiomyopathy	N/A	Med
7	72/F	Complete AV block	Cardiac sarcoidosis susp.	N/A	Med
8	74/M	Complete AV block	Secondary cardiomyopathy	N/A	Med
9	75/M	Advanced AV block	Cardiac sarcoidosis susp.	Cardiac sarcoidosis	SJM
10	78/F	Complete AV block	Cardiac sarcoidosis susp.	N/A	SJM
11	69/F	Sick sinus syndrome	Secondary cardiomyopathy	N/A	BIO
12	54/M	Complete AV block	Cardiac sarcoidosis susp.	N/A	BIO

*AV block: atrioventricular block

*Med: Advisa MRI SureScan pacemaker system (Medtronic, Inc.)

*SJM: Accent MRI™ pacemaker system (St. Jude Medical, Inc.)

*BIO: Pro MRI® pacemaker system (BIOTRONIK SE & Co.)

sarcoidosis accounts for approximately one-third of the cases of advanced atrioventricular block in middle-aged and elderly women [6].The diagnosis of cardiac involvement is difficult because the clinical manifestations are varied and nonspecific and the diagnostic rate with endomyocardial biopsy is low [15]. Recently, CMR has been found to be useful for the diagnosis of cardiac sarcoidosis, and it is now widely employed in the clinical setting [6-18]. CMR is also considered to be useful for the diagnosis of various types of cardiomyopathy and myocardial ischemia that may be responsible for arrhythmias [19-21]. The present study was conducted to assess the quality and interpretability of images acquired in CMR examinations for patients with MRI-conditional pacemakers.

Materials and Methods

Study population

The subjects in this study were 12consecutive patients (7 men and 5 women, age range:50 to 78 years, mean age: 68.4 ± 8.7 years) with MRI-conditional pacemakers who underwent CMR examinations at our institution between July 2013 and December2014.This retrospective study was approved by our institutional review board, and the requirement to obtain informed consent was waived. All subjects had implanted cardiac pacemakers for the treatment of atrioventricular block or sick sinus syndrome, and CMR was performed to assess the myocardial pathologic changes associated with the underlying diseases, which included cardiac sarcoidosis, cardiomyopathies, and ischemic heart disease. The clinical profiles of the subjects are shown in Table 1.

Seven subjects had Advisa MRI Sure Scan pacemaker systems (A3SR01) consisting of the Advisa MRI implantable pulse generator (IPG) and Capture Fix MRI leads (Medtronic, Inc., Minneapolis, MN, USA), 3 subjects had Accent MRI™ pacemaker systems consisting of the Accent MRI™ IPG and Tendril MRI™ leads (St. Jude Medical, Inc., St. Paul, MN, USA), and 2 subjects had Pro MRI pacemaker systems consisting of the Etrinsa 8 DR-T and Safio S leads (BIOTRONIKSE& Co.KG, Berlin, Germany). All pacemakers were the dual-chamber type. The IPG was implanted in the left chest in all subjects. The pacemakers were set to DOO mode (80 to 90ppm), AOO mode (80ppm), or VOO mode (60 to 100ppm) during the CMR examinations. A cardiologist and a clinical engineer with specialized training were present during all CMR examinations to deal with any unforeseeable circumstances that might arise.

CMR protocol

A 1.5-T MRI system (EXCELART Vantage™ Powered by Atlas; Toshiba Medical Systems Corporation, Otawara, Japan) and a 16-channel coil (Atlas SPEEDER Body; Toshiba) were used. The slew rate and maximum intensity of the gradient field were 200mT/m/ms and 30mT/m, respectively. The maximum spatial magnetic field gradient of the static field was 10.435 T/m (Figures 1,2).

Cine imaging for the evaluation of cardiac function

Steady-state free precession (SSFP) sequences covering the range from the cardiac base to the apex were used to acquire 2-dimensional images during breath-holding with ECG gating (repetition time [TR]/echo time [TE]: 4.2ms/2.1ms, flip angle: 73°, matrix: 192 × 256, slice thickness:10mm, and FOV:35 × 35cm). The entire heart was covered by 2-,3-,and 4-chamber long-axis and short-axis views.

Fat-suppressed black blood T2-weighted imaging for the evaluation of myocardial edema

Fast Advanced Spin Echo (FASE) sequences covering the range from the cardiac base to the apex in the end-diastolic phase were used to acquire axial 2-dimensionalmultislice images in a single breath-hold with ECG gating (repetition time [TR]/echo time[TE]:1600ms/80ms, flip angle:90°, matrix:256 × 256, slice thickness:10 mm, FOV:38 × 38cm,and BBTI: 550ms). The entire heart was covered by short-axis views.

Late gadolinium enhancement (LGE) images for the evaluation of myocardial scarring and fibrosis

Inversion recovery (IR) fast field echo (FFE) sequences covering the range from the cardiac base to the apex in the end-diastolic phase were used to acquire 3-dimensional images in approximately 20 seconds during a single breath-hold with ECG gating (repetition time [TR]/echo time[TE]:5ms/2ms, flip angle:12°, matrix:128×256, slice thickness:10mm, FOV: 35×35cm, and inversion time:220-270ms [continuously adjusted]). LGE images were acquired on average 5 to 10 minutes after the intravenous administration of gadopentetate dimeglumine (Magnevist; Bayer Healthcare, Osaka, Japan) with a contrast dose of 0.1mmol/kg. The entire heart was covered by 2- and 4-chamber long-axis and short-axis views.

Image evaluation

Two readers (K.Y. and T.K.) with more than 5 years of experience with CMR reviewed all of the image data sets and evaluated the quality of the acquired images. Image quality was semiquantitatively rated using a 4-point scale (4: sufficient for clinical diagnostic purposes, 3: not sufficient, but within the allowable range, 2: not clinically acceptable, and 1: could not be evaluated). The rating scale took into account whether the artifacts from the leads or IPG or the magnetic field in homogeneity due to the pacemaker system impaired the ability to delineate the endocardial and epicardial borders in cardiac function analysis based on observation of systolic myocardial wall motion and thickening as well as the ability to visualize the signals within the left ventricular walls for the evaluation of myocardial edema, scarring, and fibrosis. The assessment also included the uniformity within the lumens of the right and left cardiac chambers and the delineation of the atrioventricular valves (mitral valve and tricuspid valve) in 4-chamber cine images.

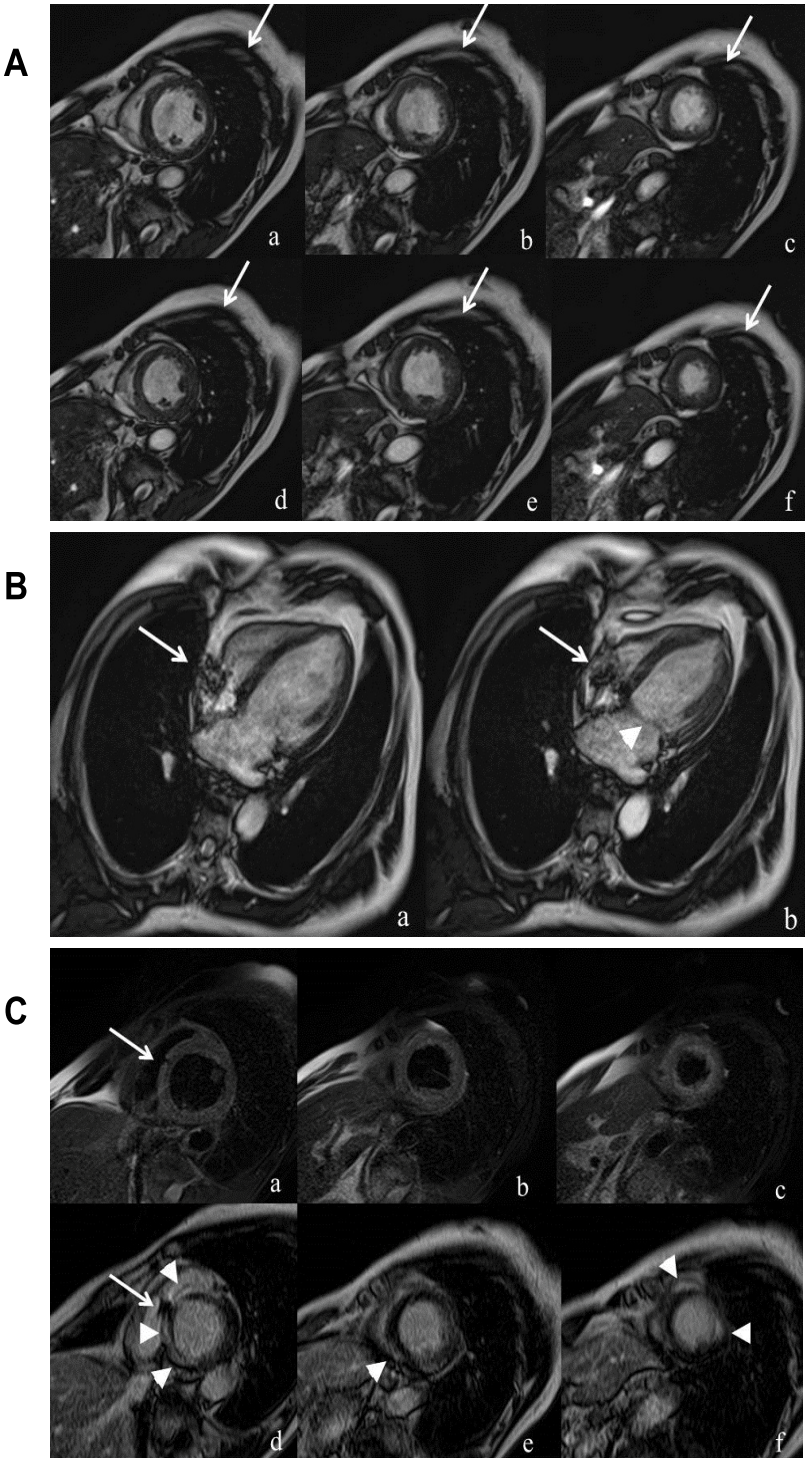

Figure1: 69-year-old man (case 2) with a dual-chamber MRI-conditional pacemaker implanted in the left chest wall.

This patient underwent CMR to identify the cause of complete atrioventricular block and was diagnosed as having cardiac sarcoidosis.

A. Short-axis cine images acquired using the SSFP technique

The upper row shows diastolic images and the lower row shows systolic images. The images on the left (a,d) are at the basal level, those in the center (b,e) are at the mid level, and those on the right (c,f) are at the apical level.

Minor IPG-related off-resonance stripe artifacts in the chest wall that do not extend to the heart (arrows) are seen. The artifacts do not interfere with the ability to delineate the right ventricular and left ventricular endocardial and epicardial borders or to evaluate cardiac function. No lead-related artifacts are observed. The result is grade 4 for all segments.

B. 4-chamber cine images acquired using the SSFP technique

Image “a” shows the diastolic phase and image “b” shows the systolic phase.

Minor susceptibility artifacts with characteristic dark signal voids (arrows) are observed around the atrial and ventricular leads. The artifacts interfere slightly with the ability to delineate the tricuspid valve (grade 2), but the mitral valve (arrowhead) can be assessed (grade 3). In addition, the signal uniformity within the right and left ventricular lumens is relatively high (grade 3).

C. Short-axis fat-suppressed black blood T2-weighted images (a,b,c) and short-axis late gadolinium enhancement (LGE) images (d,e,f)

Minor susceptibility artifacts with characteristic dark signal voids (arrows) are observed around the atrial and ventricular leads. The artifacts extend slightly into the septum at the basal level, but assessment within the myocardium is possible (grade 3). No artifacts are observed in the other segments (grade 4). In the LGE images, many contrast-enhanced spots are seen in the left-ventricular myocardium (arrowheads). These are considered to be lesions of cardiac sarcoidosis.

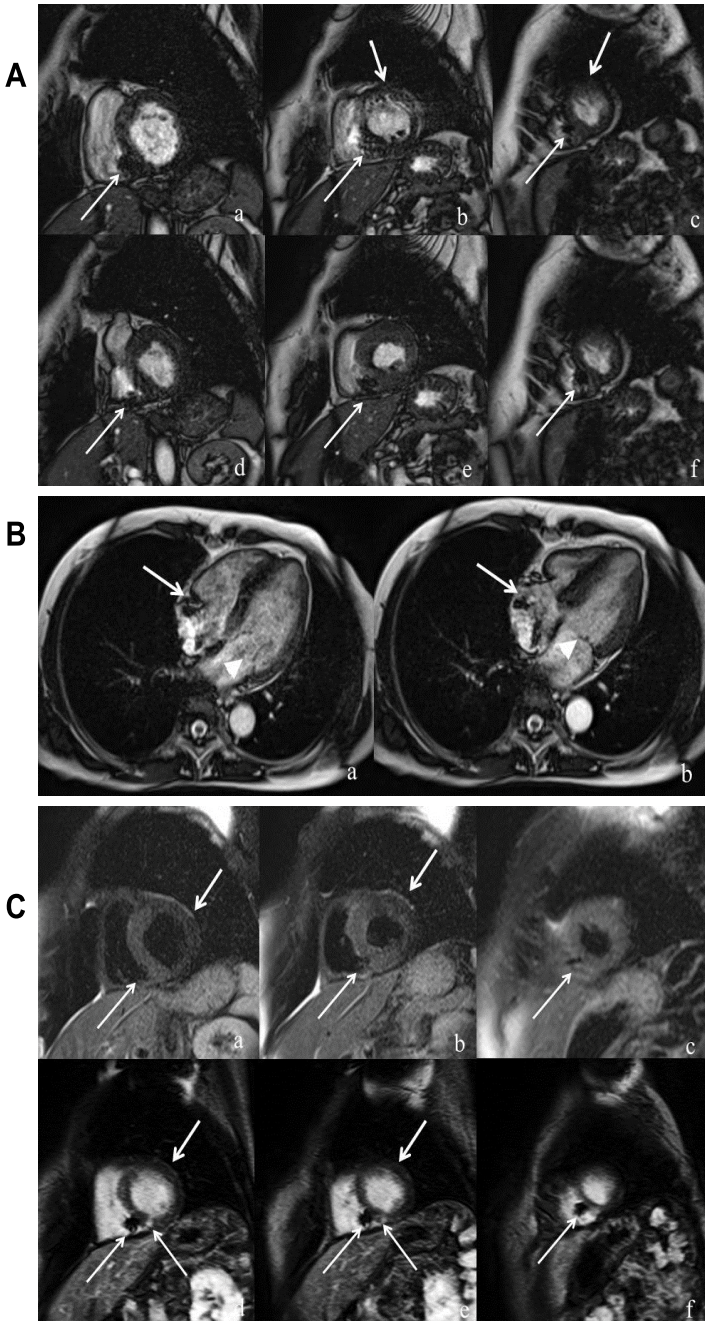

Figure 2: 67-year-old woman (case 3) with a dual-chamber MRI-conditional pacemaker implanted in the left chest wall.

This patient underwent CMR to identify the cause of complete atrioventricular block, but no obvious abnormalities were found.

A. Short-axis cine images acquired using the SSFP technique

The upper row shows diastolic images and the lower row shows systolic images. The images on the left (a,d) are at the basal level, those in the center (b,e) are at the mid level, and those on the right (c,f) are at the apical level.

Severe IPG-related off-resonance stripe artifacts are observed in the chest wall, and they extend to the anterior wall at the mid and apical levels (short arrows).

Minor susceptibility artifacts with characteristic dark signal voids (long arrows) are observed around the atrial and ventricular leads. The artifacts interfere slightly with the ability to delineate the right ventricular and left ventricular endocardial and epicardial borders and to evaluate cardiac function. The results are grade 3 for the septum at the basal level, grade 2 for all segments at the midlevel, grade 2 for the anterior wall at the apical level, and grade 3 for the septum at the apical level. For all other segments, the result is grade 4.

B. 4-chamber cine images acquired using the SSFP technique

Image “a” shows the diastolic phase and image “b” shows the systolic phase.

Minor susceptibility artifacts with characteristic dark signal voids (arrows) are observed around the atrial and ventricular leads. The artifacts interfere slightly with the ability to delineate the tricuspid valve (grade 2), but assessment of the mitral valve (arrowheads) is possible (grade 4). The signal uniformity within the right and left ventricular lumens is slightly low (grade 2).

C. Short-axis fat-suppressed black blood T2-weighted images (a,b,c) and short-axis late gadolinium enhancement (LGE) images (d,e,f)

Minor IPG-related susceptibility artifacts (short arrows) are seen in the anterior and lateral walls at the basal level and mid level (the assessment result is grade 3 for all of these segments).

Minor susceptibility artifacts with characteristic dark signal voids and bright rims (long arrows) are observed around the atrial and ventricular leads. The artifacts extend slightly into the septum at the basal, mid, and apical levels, but assessment within the myocardium is possible (the result is grade 3 for all of these segments). No artifacts are observed in the other segments grade 4.

Table 2: Visual assessment scores for the clarity of the endocardial and epicardial borders of each cardiac wall in short-axis cine images

	Anterior	Septal	Inferior	Lateral	RVFW
Basal	3.9 ± 0.3	3.5 ± 0.8	4.0 ± 0.0	3.9 ± 0.3	3.7 ± 0.7
Mid	3.8 ± 0.6	3.6 ± 0.7	3.8 ± 0.6	3.8 ± 0.6	3.8 ± 0.5
Apical	3.8 ± 0.6	3.9 ± 0.3	4.0 ± 0.0	4.0 ± 0.0	4.0 ± 0.0

(Mean ± SD), *RVFW: Right Ventricular Free Wall

Table 3: Visual assessment scores for uniformity within the right and left ventricular lumens and delineation of the mitral valve and tricuspid valve in 4-chamber cine images

Lumen	Mitral valve	Tricuspid valve
2.8 ± 0.7	3.3 ± 0.9	2.3 ± 0.7

(Mean ± SD)

Table 4: Visual assessment scores for image quality in terms ofthe artifacts from the leads and IPG that impaired the ability to evaluate the signals inside the left ventricular walls in short-axis fat-suppressed black blood T2-weighted images

	Anterior	Septal	Inferior	Lateral
Basal	3.9 ± 0.3	3.7 ± 0.5	3.9 ± 0.3	3.9 ± 0.3
Mid	3.9 ± 0.3	3.8 ± 0.5	4.0 ± 0.0	3.9 ± 0.3
Apical	4.0 ± 0.0	3.9 ± 0.3	4.0 ± 0.0	4.0 ± 0.0

(Mean ± SD)

Short-axis cine images: The clarity of the endocardial and epicardial borders, which is important for cardiac function analysis, was assessed for the left ventricular anterior, septal, inferior, and lateral walls and the right ventricular free wall at the basal, mid, and apical levels.

4-chamber cine images: Uniformity within the right and left ventricular lumens, which can be adversely affected by degradation of image quality due to magnetic field in homogeneity, was evaluated. Moreover, delineation of the mitral valve and tricuspid valve was assessed.

Short-axis fat-suppressed black blood T2-weighted images

Short-axis LGE images: Image quality in terms of the artifacts from the leads and IPG that impaired the ability to evaluate the signals within the left ventricular walls was assessed for the left ventricular anterior, septal, inferior, and lateral walls at the basal, mid, and apical levels.

Measurement of the extent of the artifacts

For the assessment of artifacts, the extent of the artifacts caused by the IPG (depth from the chest wall surface) and the size of the artifacts caused by the leads (maximum minor-axis length of the artifact) were measured in short-axis images acquired by cine imaging, fat-suppressed black blood T2-weighted imaging, and LGE imaging. The artifacts were assessed in the areas determined based on the mutual agreement of the two readers.

Results

All of the CMR examinations were performed safely and without any unexpected incidents or complications. In all subjects, the examination was completed within 45 minutes.

Image quality

Short-axis cine images: Table 2 summarizes the scores for the clarity of the endocardial and epicardial borders of each cardiac wall. The right ventricular leads were observed along the ventricular septal wall at the basal level and mid level in all subjects, and there is no much of a difference in the presence of the artifacts. In this context, the lowest score was observed for the left ventricular septal wall at the basal level (3.5 ± 0.8) and midlevel (3.6 ± 0.7) due to the presence of artifacts from the leads. Artifacts from the IPG affected the image quality of the left anterior wall in 1 of the 12 subjects (Figure 2). The borders of the left inferior and lateral walls and the right ventricular free wall were visualized with sufficient clarity for the evaluation of cardiac function.

Table 5: Visual assessment scores for image quality in terms of the artifacts from the leads and IPG that impaired the ability to evaluate the signals inside the left ventricular walls in short-axis late gadolinium enhancement images

	Anterior	Septal	Inferior	Lateral
Basal	3.8 ± 0.4	3.4 ± 0.7	4.0 ± 0.1	3.8 ± 0.6
Mid	3.8 ± 0.4	3.7 ± 0.5	4.0 ± 0.1	3.9 ± 0.3
Apical	3.9 ± 0.3	3.9 ± 0.3	4.0 ± 0.0	4.0 ± 0.0

(Mean ± SD)

Table 6: Extent of the artifacts caused by the IPG and size of the artifacts caused by the leads

	Cine	BBT2WI	LGE
IPG	87.7 ± 43.5	49.7 ± 27.4	47.1 ± 20.3
Leads	15.4 ± 6.1	9.6 ± 4.0	14.2 ± 2.7

Mean ± SD (mm)

*Cine: short-axis cine images

*BBT2WI: short-axis fat-suppressed black blood T2-weighted images

*LGE: short-axis late gadolinium enhancement images

4-chamber cine images: Table 3 summarizes the scores for the uniformity within the right ventricular lumen and the delineation of the mitral valve and tricuspid valve. The scores for the uniformity within the right and left ventricular lumens were rather poor (2.8 ± 0.7).The scores for the tricuspid valve were poor (2.3 ± 0.7), and the scores for the mitral valve showed acceptable image quality (3.3 ± 0.9).

Short-axis fat-suppressed black blood T2-weighted images: Table 4

Short-axis LGE images: Table 4 and Table 5 summarize the scores for image quality in terms of the artifacts from the leads and IPG that impaired the ability to evaluate the signals inside the left ventricular walls in short-axis fat-suppressed black blood T2-weighted images (Table 4) and short-axis LGE images (Table 5). In both images, the scores for the septum at the basal level and midlevel were slightly lower than the scores for the other segments. Artifacts from the leads affected the signals in the septum at the basal level and midlevel in almost all subjects. Compared with short-axis SSFP cine imaging, however, the influence of artifacts tended to be less severe in images acquired by fat-suppressed black blood T2-weighted imaging and LGE imaging.

Measurement of the extent of the artifacts

Table 6 summarizes the extent of the artifacts caused by the IPG and the size of the artifacts caused by the leads. The artifacts from the IPG and from the leads were most severe in SSFP cine images as compared with fat-suppressed black blood T2-weighted images and LGE images.

Discussion

MRI requires a high-strength static magnetic field and powerful radiofrequency and gradient magnetic fields. These requirements are associated with both theoretical and observed risks due to their effects on CIEDs [14,22]. The first risk is the induction of electrical currents. This risk results from the radiofrequency and gradient magnetic fields [23]. There is concern that the induced currents could lead to rapid asynchronous pacing and associated hemodynamic compromise. The second risk is interference with device function. The static, radiofrequency, and gradient magnetic fields can all interact with the circuitry of the device. These interactions have the potential to temporarily or permanently affect device function and may result in inappropriate sensing, triggering, activation, or resetting of the device. The third risk is mechanical force [24]. The static magnetic field exerts forces on certain metals. CIEDs contain small amounts of these metals, making them weakly ferromagnetic. As a result, there is a possibility that these devices may migrate when placed in the scanner because they are attracted to the magnet. A 6-week interval between device implantation and MRI examination is recommended in order to allow fibrosis encapsulation of the leads and IPG [25]. The

last risk is lead heating. The radiofrequency field can cause heating at the lead-myocardial interface. However, an *in vivo* canine study reported that heating at the lead tip was minimal when a clinical MRI protocol was used [14]. It has been suggested that the cooling effect of blood flow through the heart may be a protective factor.

Despite the above concerns, several studies have demonstrated that patients with CIEDs can safely undergo MRI examinations under close supervision [26-28]. However, nearly all CIEDs are currently considered to be a contraindication to MRI. In 2011, the Revo MRI Sure Scan pacemaker system (Medtronic, Inc.) was approved by the FDA in the United State as an MRI-conditional device, and approval of the Advisa MRI Sure Scan pacemaker system (Medtronic, Inc.) followed in 2013. In Japan, the first MRI-conditional pacemaker was the Advisa MRI Sure Scan pacemaker system, which was introduced in October 2012, and many MRI-conditional CIEDs are currently available. The term "MRI-conditional" refers to a lack of known hazards if a certain set of conditions are met. For these devices, the initial conditions included a maximum gradient slew rate of <200T/m/s, a whole-body specific absorption rate (SAR) of <2W/kg, and a head SAR of <3.2W/kg (normal operating mode).

The SSFP technique is the most widely employed scanning method in routine clinical CMR examinations. With an SSFP pulse sequence, the entire heart is typically covered by cine 2-, 3-, and 4-chamber long-axis and short-axis views. Short-axis views are most frequently used for the evaluation of chamber volumes, ejection fraction, wall motion, and myocardial remodeling. In order to evaluate these parameters in short-axis views, it is necessary to trace the endocardial and epicardial borders in the range from the base to the apex manually or semi-automatically using a workstation. The clarity of the endocardial and epicardial borders of each cardiac wall is therefore very important.

In the visual assessment of the clarity of the endocardial and epicardial borders of each cardiac wall in short-axis cine images, the scores for the left ventricular septal wall at the basal level and midlevel were relatively low due to the presence of artifacts from the leads. In addition, artifacts from the IPG affected the image quality of the left anterior wall in 3 of the 12 subjects, and the image quality was quite poor in 1 of these 3 subjects. The reason of this fact was unknown and was considered to be unrelated with body size of this subject.

In the assessment of the extent of the artifacts caused by the IPG and the size of the artifacts caused by the leads, the artifacts were found to be larger in the short-axis SSFP cine images than in the short-axis fat-suppressed black blood T2-weighted images or short-axis LGE images. The SSFP technique is one of the most sensitive scanning methods with regard to local field in homogeneities that can occur in patients with metallic or electronic implants. Although local field in homogeneities did cause local artifacts along the leads, many MRI-conditional CIEDs incorporate modifications to ensure safety; for example, the leads are modified to reduce RF heating and the amount of ferromagnetic materials is limited. These modifications may have reduced the level of artifacts observed, but it is not possible to report proof for such mechanisms.

Schwitter et al. have reported the results of the Advisa MRI randomized clinical multicenter study to evaluate CMR image quality for SSFP cine images and tagging CMR [5]. In their study, cine SSFP acquisitions yielded good to excellent image quality for the left ventricle and right ventricle in most cases, and only 5% of the left ventricular MR acquisitions and 2% of the right ventricular MR acquisitions were of nondiagnostic quality. In our study, the influence of artifacts on the cardiac walls was also localized, and the artifacts did not have a severe impact on the evaluation of cardiac function.

The results for the visual assessment of the uniformity within the right and left ventricular lumens in 4-chamber cine images were rather poor, and some deterioration attributable to magnetic field in homogeneity was observed. However, this result did not appear to affect the evaluation of cardiac function.

Regarding the delineation of the mitral valve and tricuspid valve, the scores for the mitral valve showed that it was visualized with acceptable image quality, but the scores for the tricuspid valve were poor. It is considered that artifacts along the lead running from the right atrium to the right ventricle, which were caused by local field in homogeneity, strongly affected the delineation of the tricuspid valve.

Concerning the results for image quality in short-axis fat-suppressed black blood T2-weighted images and short-axis LGE images, the scores for the septum at the basal level and midlevel were slightly lower than the scores for the other segments. Artifacts from the leads affected the signals in the septum at the basal level and midlevel in almost all subjects. Compared with short-axis SSFP cine imaging, however, the influence of artifacts tended to be less severe in images acquired by fat-suppressed black blood T2-weighted imaging and LGE imaging.

It should be noted, however, that although lead-induced artifacts in the septum at the basal level and midlevel did not present problems for the subjects in the present study, the lesions of cardiac sarcoidosis are frequently located in these areas. It is therefore expected that cases in which artifacts from the leads interfere with the diagnosis of cardiac sarcoidosis will be encountered in the future as the number of cases examined by CMR increases [6,17].

Our study has several limitations. First and most important, the number of subjects is small. A multicenter trial will be necessary for the evaluation of a substantial number of patients. Second, the visual scoring of image quality is subjective and does not permit quantitative analysis. Third, we used only a single MRI scanner and only a single type of scan sequence which we employ for routine examinations. Susceptibility artifacts are typically suppressed by reducing the TE, increasing the bandwidth, increasing the resolution in the phase direction, and employing spin echo sequences rather than gradient echo sequences. In the future, it will be necessary to develop sequences and scan parameters that reduce artifacts. However, cardiac MRI requires high temporal resolution and other stringent imaging conditions, and it may therefore be difficult to eliminate the influence of artifacts completely.

Conclusion

CMR can be performed safely in patients with MRI-conditional pacemakers, and image quality and interpretability are acceptable for the analysis of cardiac function as well as the evaluation of myocardial edema, scarring, and fibrosis, although some deterioration in uniformity within the lumens of the cardiac chambers due to magnetic field in homogeneity and artifacts from the leads and from the IPG may be observed.

References

1. Martin ET, Coman JA, Shellock FG, Pulling CC, Fair R, et al. (2004) Magnetic resonance imaging and cardiac pacemaker safety at 1.5-Tesla. J Am Coll Cardiol 43: 1315-1324.
2. Brown DW, Croft JB, Giles WH, Anda RF, Mensah GA (2005) Epidemiology of pacemaker procedures among Medicare enrollees in 1990, 1995, and 2000. Am J Cardiol 95: 409-411.
3. Moss AJ, Zareba W, Hall WJ, Klein H, Wilber DJ, et al. (2002) Prophylactic implantation of a defibrillator in patients with myocardial infarction and reduced ejection fraction. N Engl J Med 346: 877-883.
4. Kalin R, Stanton MS (2005) Current clinical issues for MRI scanning of pacemaker and defibrillator patients. Pacing Clin Electrophysiol 28: 326-328.
5. Schwitter J, Kanal E, Schmitt M, Anselme F, Albert T, et al. (2013) Impact of the Advisa MRI system on the diagnostic quality of cardiac MR images and contraction patterns of cardiac muscle during scans: Advisa MRI randomized clinical multicenter study results. Heart Rhythm 10: 864-872.
6. Yoshida Y, Morimoto S, Hiramitsu S, Tsuboi N, Hirayama H, et al. (1997) Incidence of cardiac sarcoidosis in Japanese patients with high-degree atrioventricular block. Am Heart J 134: 382-386.
7. Shellock FG, Crues JV (2004) MR procedures: biologic effects, safety, and patient care. Radiology 232: 635-652.
8. Prasad SK, Pennell DJ (2004) Safety of cardiovascular magnetic resonance in patients with cardiovascular implants and devices. Heart 90: 1241-1244.
9. Faris OP, Shein MJ (2005) Government viewpoint: U.S. Food & Drug Administration: Pacemakers, ICDs and MRI. Pacing Clin Electrophysiol 28: 268-269.

10. Nazarian S, Roguin A, Zviman MM, Lardo AC, Dickfeld TL, et al. (2006) Clinical utility and safety of a protocol for noncardiac and cardiac magnetic resonance imaging of patients with permanent pacemakers and implantable-cardioverter defibrillators at 1.5 tesla. Circulation 114: 1277-1284.

11. Smith JM (2005) Industry viewpoint: Guidant: Pacemakers, ICDs, and MRI. Pacing Clin Electrophysiol 28: 264.

12. Stanton MS (2005) Industry viewpoint: Medtronic: Pacemakers, ICDs, and MRI. Pacing Clin Electrophysiol 28: 265.

13. Levine PA (2005) Industry viewpoint: St. Jude Medical: Pacemakers, ICDs and MRI. Pacing Clin Electrophysiol 28: 266-267.

14. Shinbane JS, Colletti PM, Shellock FG (2011) Magnetic resonance imaging in patients with cardiac pacemakers: era of "MR Conditional" designs. J Cardiovasc Magn Reson 13: 63.

15. Uemura A, Morimoto S, Hiramitsu S, Kato Y, Ito T, et al. (1999) Histologic diagnostic rate of cardiac sarcoidosis: evaluation of endomyocardial biopsies. Am Heart J 138: 299-302.

16. Smedema JP, Snoep G, van Kroonenburgh MP, van Geuns RJ, Dassen WR, et al. (2005) Evaluation of the accuracy of gadolinium-enhanced cardiovascular magnetic resonance in the diagnosis of cardiac sarcoidosis. J Am Coll Cardiol 45: 1683-1690.

17. Tadamura E, Yamamuro M, Kubo S, Kanao S, Saga T, et al. (2005) Effectiveness of delayed enhanced MRI for identification of cardiac sarcoidosis: comparison with radionuclide imaging. AJR Am J Roentgenol 185: 110-115.

18. Greulich S, Deluigi CC, Gloekler S, Wahl A, Zürn C, et al. (2013) CMR imaging predicts death and other adverse events in suspected cardiac sarcoidosis. JACC Cardiovasc Imaging 6: 501-511.

19. Rutz AK, Manka R, Kozerke S, Roas S, Boesiger P, et al. (2009) Left ventricular dyssynchrony in patients with left bundle branch block and patients after myocardial infarction; integration of mechanics and viability by CMR. Eur Heart J 30: 2117-2127.

20. Simpson RM, Keegan J, Firmin DN (2013) MR assessment of regional myocardial mechanics. J Magn Reson Imaging 37: 576-599.

21. Manka R, Kozerke S, Rutz AK, Stoeck CT, Boesiger P, et al. (2012) A CMR study of the effects of tissue edema and necrosis on left ventricular dyssynchrony in acute myocardial infarction: implications for cardiac resynchronization therapy. J Cardiovasc Magn Reson 14: 47.

22. Martin ET (2005) Can cardiac pacemakers and magnetic resonance imaging systems co-exist? Eur Heart J 26: 325-327.

23. Shellock FG, Tkach JA, Ruggieri PM, Masaryk TJ (2003) Cardiac pacemakers, ICDs, and loop recorder: evaluation of translational attraction using conventional ("long-bore") and "short-bore" 1.5- and 3.0-Tesla MR systems. J Cardiovasc Magn Reson 5: 387-397.

24. Fisher JD (2005) MRI: safety in patients with pacemakers or defibrillators: is it prime time yet? Pacing Clin Electrophysiol 28: 263.

25. Faris OP, Shein M (2006) Food and Drug Administration perspective: Magnetic resonance imagingof pacemaker and implantable cardioverter-defibrillator patients. Circulation 114: 1232-1233.

26. Burke PT, Ghanbari H, Alexander PB, Shaw MK, Daccarett M, et al. (2010) A protocol for patients with cardiovascular implantable devices undergoing magnetic resonance imaging (MRI): should defibrillation threshold testing be performed post-(MRI). J Interv Card Electrophysiol 28: 59-66.

27. Buendía F, Sánchez-Gómez JM, Sancho-Tello MJ, Olagüe J, Osca J, et al. (2010) Nuclear magnetic resonance imaging in patients with cardiac pacing devices. Rev Esp Cardiol 63: 735-739.

28. Cohen JD, Costa HS, Russo RJ (2012) Determining the risks of magnetic resonance imaging at 1.5 tesla for patients with pacemakers and implantable cardioverter defibrillators. Am J Cardiol 110: 1631-1636.